Functions of leptin in tuberculosis and diabetes: multi-omics studies across species

Ding, Y.

Citation

Ding, Y. (2021, December 7). *Functions of leptin in tuberculosis and diabetes: multi-omics studies across species*. Retrieved from https://hdl.handle.net/1887/3245305

Chapter

5

Leptin mutation and mycobacterial infection leads non-synergistically to a similar metabolic syndrome

Yi Ding[1], Mariëlle C Haks[2], Tom H. M. Ottenhoff[2], Amy C. Harms[3], Thomas Hankemeier[3], Muhamed N. H. Eeza[4, 5], Jörg Matysik[4], A. Alia[5,6], Herman P. Spaink[1*]

[1] Institute of Biology, Leiden University, The Netherlands

[2] Department of Infectious Diseases, Leiden University Medical Center, The Netherlands

[3] Leiden Academic Centre for Drug Research, Leiden University, The Netherlands

[4] Institute of Analytical Chemistry, University of Leipzig, Linnéstraße 3, D-04103, Leipzig, Germany

[5] Institute for Medical Physics and Biophysics, University of Leipzig, 04107 Leipzig, Germany.

[6] Leiden Institute of Chemistry, Leiden University, 2333 Leiden, The Netherlands.

*Corresponding author, email: h.p.spaink@biology.leidenuniv.nl

Manuscript in preparation

131

ABSTRACT

The leptin signaling pathway, originally discovered as one of the major factors that controls food intake, has been subsequently shown to play an evolutionary conserved role in regulating glucose homeostasis and system metabolism. Furthermore, it plays an important role as a key regulator of cellular and systemic inflammatory responses. In accordance, the leptin gene plays a role in many diseases such as cancer, tuberculosis and diabetes. In this study, we investigated the metabolism of a leptin mutant in the absence and presence of mycobacterial infection in mice and zebrafish larvae. Metabolites in the blood of *ob/ob* mice and entire *lepb* mutant zebrafish larvae were studied using mass spectrometry and HR-MAS NMR spectrometry, respectively. The results show that leptin mutation leads to a similar metabolic syndrome as caused by mycobacterial infection in the two species, characterized by the decrease of 11 amine metabolites. In both species, this metabolic syndrome is not aggravated when the leptin mutant is infected by mycobacteria. Therefore, we conclude that leptin and mycobacterial infection are both impacting metabolism non-synergistically. In addition, we studied the transcriptomes of *lepb* mutant zebrafish larvae and wild type siblings after mycobacterial infection. The transcriptome studies in zebrafish larvae show that mycobacteria induce a very distinct transcriptome signature in the *lepb* mutant compared to the wild type sibling control. Apparently, different transcriptomic responses can lead to the same metabolic end states.

Introduction

Tuberculosis (TB) is an infectious disease which causes around 10 million cases and 1.2 million deaths reported to the World Health Organization in 2019 [1]. Approximately one quarter of the world's population is latently infected with *Mycobacterium tuberculosis (Mtb)*, the causative agent of TB [1]. In around 10% of these latent infections progresses to active TB disease [2]. TB is often associated with severe wasting syndrome accompanied by loss of whole body mass and increased risk of death [3]. The metabolic abnormalities underlying the wasting syndrome in TB have been studied in humans and TB animal models [4, 5]. TB causes metabolic reprogramming characterized by decrease of many metabolites in the blood of patients from Africa [4], China [6], Indonesia [7] and the Netherlands [5]. The metabolic responses towards mycobacterial infection in the blood of mice are highly similar to that in TB patients [5]. We have shown that even in entire zebrafish larvae, infection with *M. marinum*, a natural fish pathogen and a close relative of *Mtb*, leads to a very similar metabolic syndrome as observed in mice and patients after infection with *Mtb* [5]. Ten small amines were identified as common biomarkers of mycobacterial infection in TB patients, mice and zebrafish larvae [5].

One of the risk factors for the development of TB is type 2 diabetes mellitus (T2DM) [8]. T2DM patients are three times more likely to develop progressive tuberculosis infection than normoglycemic people [9]. TB accompanied by T2DM leads to higher *Mtb* bacillary loads in sputum compared with TB patients without T2DM [10]. This might be due to the defects in the immune responsiveness in diabetic patients [11]. Alternatively, the changes in system metabolism associated with T2DM could lead to a higher risk of TB [12]. Interestingly, both TB and T2DM can lead to a similar metabolic syndrome that is companied by muscle wasting [12, 13]. Mouse and zebrafish mutants in leptin signaling genes are used to study metabolic alterations associated with T2DM [14-17]. These studies have shown that leptin in addition to its function in controlling of food intake plays an evolutionarily conserved role in regulating glucose homeostasis [16, 17]. Leptin has also been shown to have a function in mediating a glucose-fatty acid cycle to maintain glucose homeostasis under starvation condition in rats [18]. We previously find that leptin deficiency causes similar metabolite alterations in both mice and zebrafish larvae [19]. These metabolic changes show similar features as observed during progression of tuberculosis in human patients, mice and zebrafish larvae [19]. Studies in a mouse leptin mutant have provided evidence that leptin plays a role in the early immune response to *Mtb* infection [20]. Several studies have shown a correlation between the serum level of leptin and the risk of acquiring active TB [21-24]. The function of leptin in the susceptibility of TB and T2DM is linked to the important role of leptin as a major player in inflammatory processes and to its function as a regulator of system metabolism [7, 25]. However, the connections between the mechanisms underlying the role of leptin in TB and T2DM are still unknown.

In this study, we investigated the metabolic response in leptin mutants in the absence and presence of mycobacterial infection in mice and zebrafish larvae. We compared the effects of mycobacterial infection in the leptin mutant zebrafish larvae and mice using metabolomics. Our results showed that leptin mutations and mycobacterial infection led to a similar metabolic syndrome. This metabolic syndrome, however, was not more severe after mycobacterial infection in the leptin mutant. Subsequent transcriptome studies in zebrafish larvae showed that mycobacteria induced a very distinct transcriptome signature in the leptin mutant compared to the wild type sibling control. Apparently, different transcriptomic responses can lead to the same metabolic end states. Therefore, we conclude that leptin and mycobacterial infection control metabolism in different ways despite share metabolic features.

Results

Measurement of bacterial burden and metabolic profiles of *lepb* mutant and control zebrafish larvae in the absence and presence of *M. marinum* infection.

Lepb mutant (*lepb*$^{-/-}$) zebrafish larvae and their wild type siblings (*lepb*$^{+/+}$) were injected in the yolk with mWasabi-labeled *M. marinum* strain M or mock-injected with 2% polyvinylpyrrolidone 40 (PVP 40) at 4 hours post fertilization (hpf). Images of the four groups of zebrafish larvae were acquired at 5 days post infection (dpi) and the representative images are shown in **Figure 1A**. The images showed that most bacteria after *M. marinum* infection in both *lepb*$^{+/+}$ and *lepb*$^{-/-}$ larvae were present in yolk but were also detectable in the tail (**Figure 1A**). Pixel count quantification of bacterial burden in entire larvae was significantly higher in the *lepb*$^{-/-}$ infected zebrafish larvae than in the *lepb*$^{+/+}$ siblings (**Figure 1B).** Metabolic profiles of the four groups of pooled zebrafish larvae were measured by high-resolution magic-angle-spinning nuclear magnetic resonance (HR-MAS NMR) spectroscopy. A partial least squares discriminant analysis (PLS-DA) scores plot on the metabolic profiles of zebrafish larvae showed three separate clusters (**Figure 1C**). The *lepb*$^{+/+}$ infected cluster overlapped with the other three clusters (**Figure 1C**). The HR-MAS NMR spectra were divided into two major regions: 0.8-4.4 ppm and 6.7-8.2 ppm. Peak assignment was performed according to earlier literature and the chemical shift of the metabolites in the HMDB database (**Figure 1D**). There were 27 metabolites assigned, including alanine, lysine, lactate and phenylalanine (**Figure 1D**). The fold change and *p* value of all the measured metabolites in different comparisons were shown in **Supplementary Table S1**.
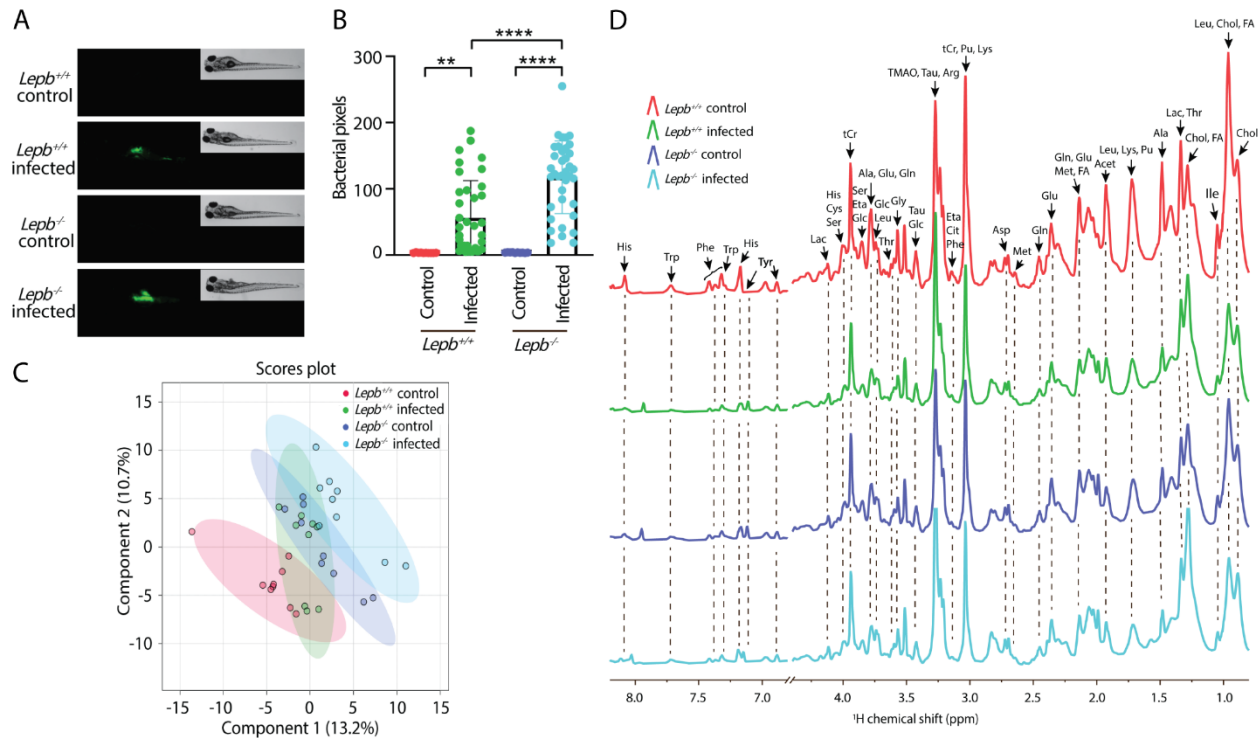
Figure 1. Bacterial loads and metabolic profiles of *lepb*⁺/⁺ and *lepb*⁻/⁻ zebrafish larvae with and without *M. marinum* infection. A. Representative bright field and fluorescent images of 5dpf zebrafish larvae from the *lepb*⁺/⁺ and *lepb*⁻/⁻ group in the absence and presence of infection. **B**. Quantifications of bacterial pixels of the four groups. **p<0.01, ****p<0.0001. **C**. PLS-DA analysis of metabolic profiles from the four groups. PLS-DA: Partial least square discriminant analysis. **D**. The representative HR-MAS NMR spectra of the four groups. Acet: acetate, Ala: alanine, Arg: arginine, Asp: aspartate, Chol: cholesterol, Cit: citrulline, Cys: cysteine, Eta: ethanolamine, FA: fatty acid, Glc: Glucose, Gln: glutamine, Glu: glutamate, Gly: glycine, His: Histidine, Ile: isoleucine, Lac: lactate, Leu: leucine, Lys: lysine, Met: methionine, Phe: phenylalanine, Pu: putrescine, Ser: serine, Tau: taurine, Thr: threonine, tCr: total creatine (creatine + phosphocreatine), Trp: Tryptophan, Tyr: tyrosine, NMR: Nuclear magnetic resonance.

Mutation of the *lepb* gene and *M. marinum* infection lead non-synergistically to a similar metabolic syndrome in zebrafish larvae

Firstly, we compared the result of the wild type *M. marinum* infection in our current HR-MAS NMR study with previously published infection in zebrafish larvae using solution NMR [5] (**Supplementary Figure S1**). The result showed 20 common metabolites in the two data sets, confirming most of the previously reported biomarkers for infection in zebrafish larvae (**Supplementary Figure S1**). Secondly, we generated Venn diagrams to compare the metabolic effects of infection in the *lepb* mutant compared to the wild type sibling control at a *p* value <0.05 with and without applying a 1.5-fold change (FC) filter. The Venn diagrams of **Figure 2A** and **2C** showed that the number of metabolites of which the levels were changed after infection in the *lepb*⁻

$^{/-}$ mutant was lower than in the *lepb*$^{+/+}$ sibling control (**Figure 2C** and **2E**). The Venn diagrams of **Figure 3A** and **3B** showed that the number of metabolites of which the levels were different between the *lepb* mutant and wild type in the absence of infection was much higher than in the presence of infection. As can be seen in **Figure 2E** and **3D**, this is the consequence of many of the metabolite levels decreasing in response to infection in the wild type were already decreased in the absence of infection in the mutant compared to the wild type. In conclusion, infection in the *lepb* mutant does not lead to lowering of the levels of the infection biomarker metabolites. Therefore, we can conclude that there is no clear synergy of the effects of *lepb* mutation and *M. marinum* infection on metabolism. The *lepb* mutation, therefore, does not exacerbate the metabolic wasting syndrome caused by *M. marinum* infection. However, there were a few metabolite levels that were specifically changing in the mutant after infection. The level of a metabolite namely lactate was specifically higher in the mutant group after infection while it was lower in the wild type after infection (**Figure 2A** and **2B**). Two other metabolites, trimethylamine N-oxide and mannose had a higher level in the *lepb*$^{-/-}$ than *lepb*$^{+/+}$ zebrafish larvae after infection (**Figure 2D** and **Figure 3C**).
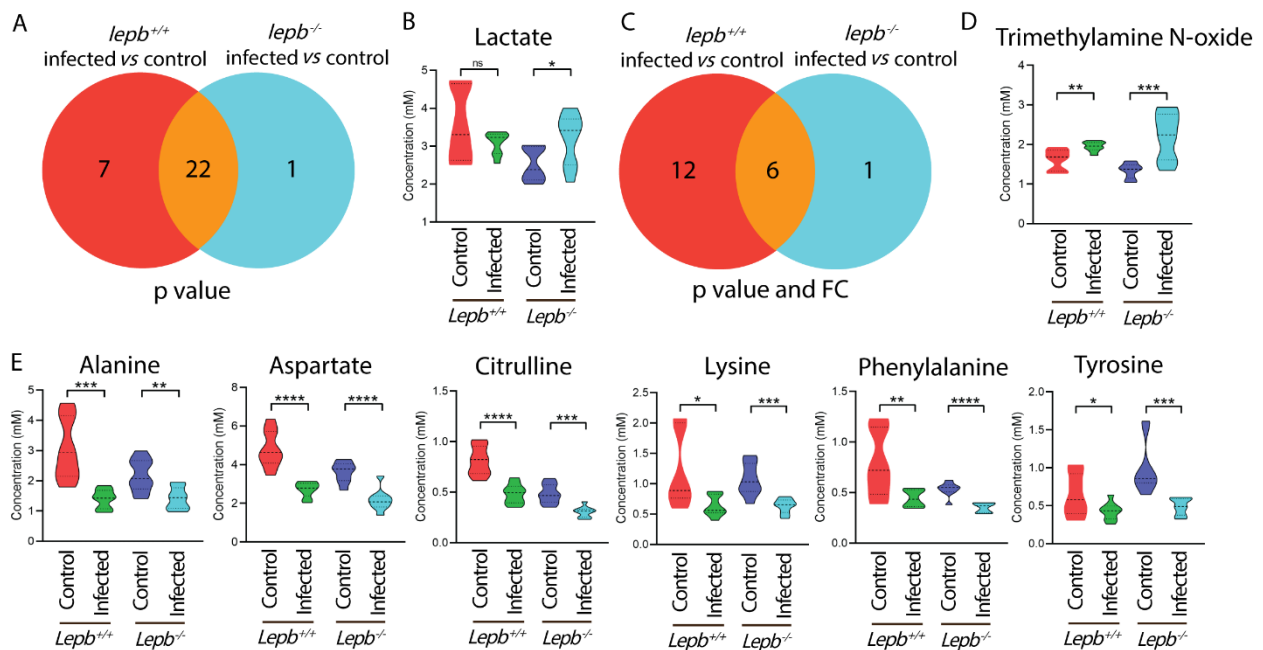
Figure 2. Venn diagrams show the number of metabolites in response to infection in the *lepb*$^{+/+}$ and *lepb*$^{-/-}$ zebrafish larvae. A. A Venn diagram shows the number of metabolites in response to *M. marinum* infection in the *lepb*$^{+/+}$ and *lepb*$^{-/-}$ larvae with $p<0.05$. **B**. Quantification of the one metabolite lactate in Figure 2A. *$p<0.05$. ns, non-significant. **C.** A Venn diagram shows the number of metabolites in response to *M. marinum* infection in the *lepb*$^{+/+}$ and *lepb*$^{-/-}$ larvae with $p<0.05$ and $|FC|>1.5$. FC: fold change. **D**. Quantification of the one metabolite trimethylamine N-oxide in Figure 2C. **$p<0.01$, ***$p<0.001$. **E**. Quantification of the common 6 metabolites in Figure 2C. ****$p<0.0001$.
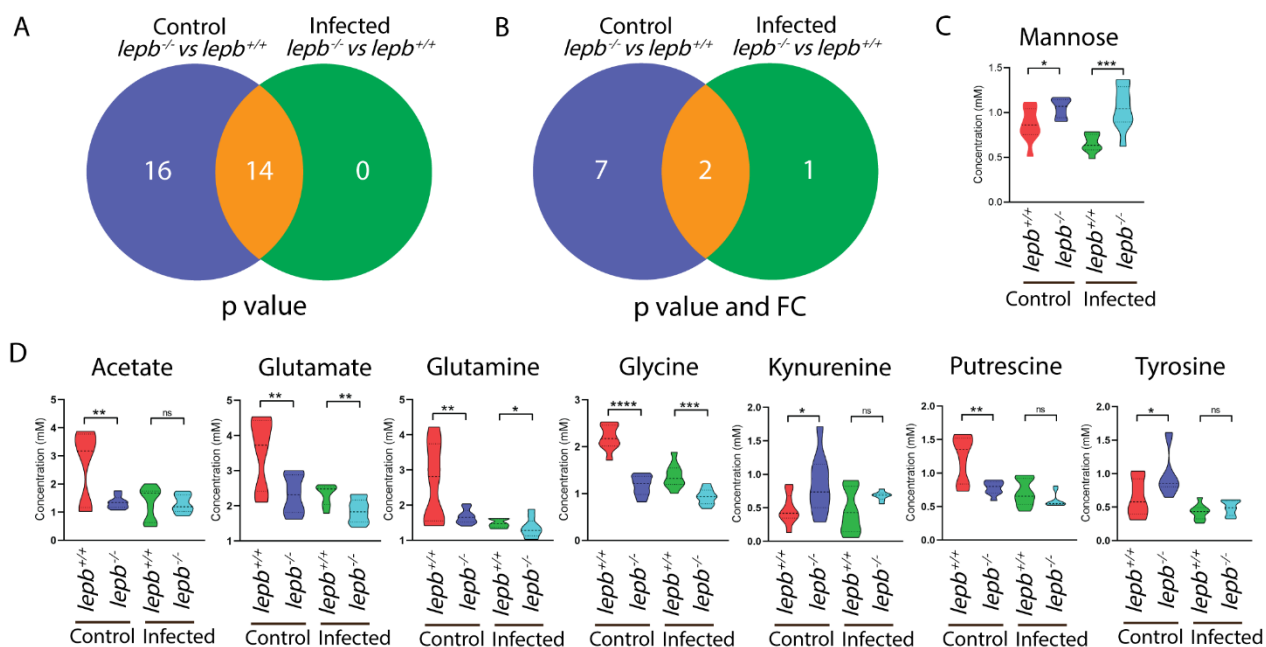
Figure 3. Venn diagrams show the number of metabolites between the _lepb^-/-_ and _lepb^+/+_ in the uninfected control and infected conditions. A. A Venn diagram shows the number of metabolites between the _lepb^-/-_ and _lepb^+/+_ in the uninfected control and infected conditions with $p<0.05$. **B**. A Venn diagram shows the number of metabolites between the _lepb^-/-_ and _lepb^+/+_ in the uninfected control and infected conditions with $p<0.05$ and $|FC|>1.5$. FC: fold change. **C**. Quantification of the one metabolite mannose in Figure 3B. *$p<0.05$, ***$p<0.001$. **D**. Quantification of the seven metabolites in Figure 3B. **$p<0.01$, ****$p<0.0001$. ns, non-significant.

Metabolic profiles of the blood of leptin mutant _ob/ob_ and wild type mice in the absence and presence of _Mtb_ infection.

Leptin deficient _ob/ob_ mice and lean C57BL/6 mice, as a wild type control, were nasally infected with _M. tuberculosis (Mtb)_. After 8 weeks, the lungs and spleens were collected and were analyzed for bacterial colony-forming unit (CFU). Plating of bacteria from the isolated organ materials showed that the mice were systemically infected by _Mtb_ in both _ob/ob_ and wild type mice (**Figure 4A** and **B**). There was more infection in the lungs of _ob/ob_ mice than that in the wild type mice, but not in the spleen (**Figure 4A** and **B**). The metabolic profiles of the blood of these mice were measured by mass spectrometry (MS). A PLS-DA scores plot showed that the data sets of the _ob/ob_ and wild type mice could be separated based on two principal components (**Figure 4C**). However, the control and infected data sets were not be completely separated in the _ob/ob_ and wild type mice (**Figure 4C**). A heatmap showed the abundances of 41 metabolites which were significantly changed in the comparison of infected versus uninfected in the two groups of mice (**Figure 4D**). It reveals that the levels of a majority of those metabolites were reduced in the wild type mice after

Mtb infection (**Figure 4D**). The levels of the metabolites in *ob/ob* mice were not obviously altered due to infection (**Figure 4D**).
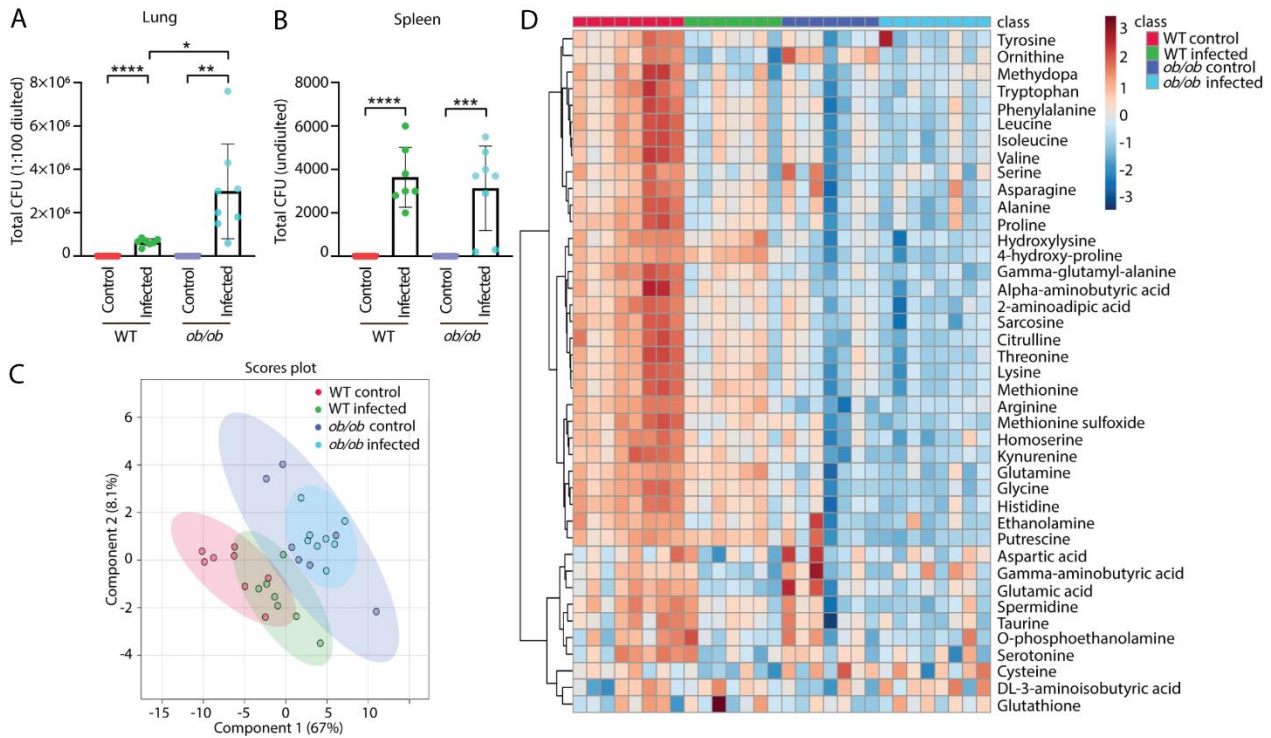


Figure 4. Bacterial loads and metabolic profiles of the blood of wild type and *ob/ob* mice with and without *Mtb* infection. A. Total CFU (1:100 diluted) of the lungs from the WT and *ob/ob* mice in the absence and presence of infection. CFU: colony-forming unit. WT: wild type. *$p<0.05$,**$p<0.01$, ****$p<0.0001$. **B**. Total CFU (undiluted) of the spleen from the four groups. ***$p<0.001$. **C**. PLS-DA analysis of the blood metabolic profiles of the four groups. PLS-DA: Partial least square discriminant analysis. **D**. Heatmap analysis of the four groups.

Mutation of the leptin gene and *Mtb* infection lead non-synergistically to a similar metabolic syndrome in mice

Venn diagrams were generated to compare the metabolic effect of infection in the *ob/ob* mutant mice as compared to the wild type control at a *p* value <0.05 with and without applying a 1.5-FC filter. The Venn diagrams of **Figure 5A** and **5D** showed that the number of metabolites of which the levels were changed after infection in the *ob/ob* mutant mice was much lower than in the wild type control. After applying 1.5-FC filter, only one metabolite, namely ornithine, was commonly lower after infection in both wild type and *ob/ob* mice (**Figure 5C**). The Venn diagrams of **Figure 6A** and **6B** showed that the number of metabolites of which the levels were different between the *ob/ob* mutant and wild type in the absence of infection was higher than in the presence of infection.

This is because the concentrations of a majority of the metabolites were decreased already as a result of leptin mutation compared to wild type mice. *Mtb* infection thus did not enhance the metabolic effects of leptin mutation. In conclusion, infection in the *ob/ob* mutant does not lead to lowering of the levels of the infection biomarker metabolites. Therefore, we conclude there is no clear synergy of the effects of leptin mutation and *Mtb* infection on metabolism. The leptin mutation, therefore, does not exacerbate the metabolic wasting syndrome caused by *Mtb* infection. However, two metabolites 3-aminoisobutyric acid and putrescine were significantly changed in *ob/ob* mice but not in wild type mice after infection (**Figure 5B** and **6C**). Although arginine levels were lower as a result of *Mtb* infection in the wild type, they were higher in the *ob/ob* mice (**Figure 5C**).
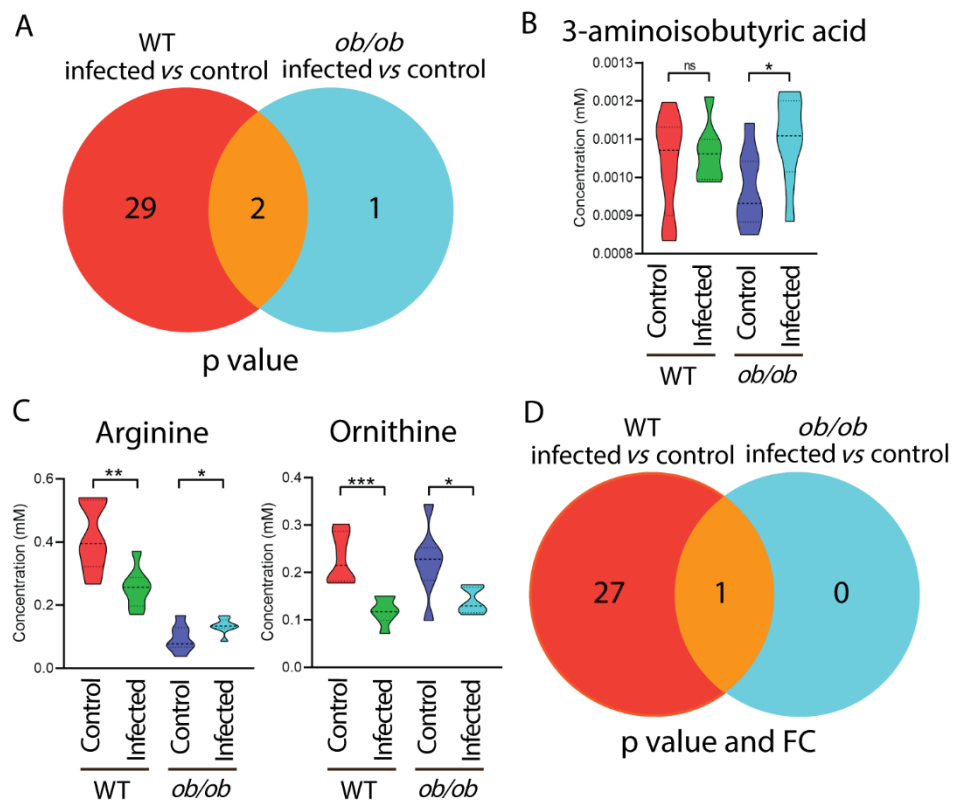
Figure 5. Venn diagrams show the number of metabolites in response to infection in the wild type and *ob/ob* mice. A. A Venn diagram shows the number of metabolites in response to *Mtb* infection in the WT and *ob/ob* mice with $p<0.05$. WT, wild type. **B**. Quantification of the one metabolite 3-aminoisobutyric acid in Figure 5A. *$p<0.05$. ns, non-significant. **C.** Quantification of the two common metabolites arginine and ornithine in Figure 5A. *$p<0.05$,**$p<0.01$, ***$p<0.001$. **D.** A Venn diagram shows the number of metabolites in response to *Mtb* infection in the wild type and *ob/ob* mice with $p<0.05$ and $|FC|>1.5$. FC: fold change.
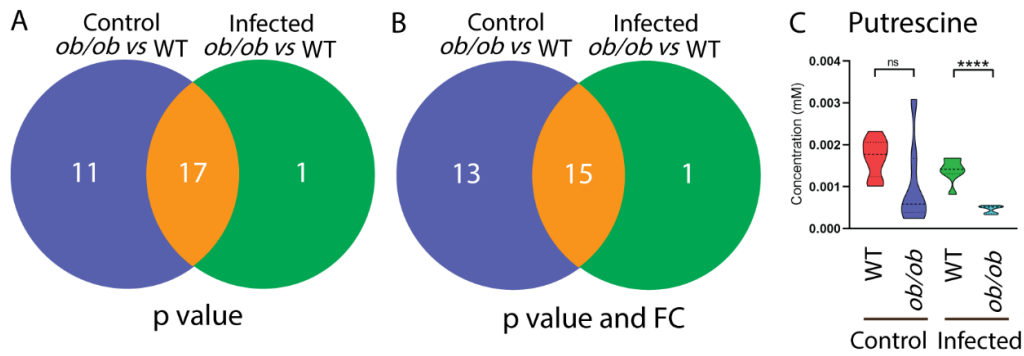
Figure 6. Venn diagrams show the number of metabolites between the wild type and *ob/ob* mice in the uninfected control and infected conditions. A. A Venn diagram shows the number of metabolites between the WT and *ob/ob* mice in the uninfected control and infected conditions with $p<0.05$. WT, wild type. **B**. A Venn diagram shows the number of metabolites between the WT and *ob/ob* mice in the uninfected control and infected conditions with $p<0.05$ and $|FC|>1.5$. FC: fold change. **C**. Quantification of the one metabolite putrescine in Figure 6A and B. ****$p<0.0001$. ns, non-significant.

The metabolic syndrome caused by leptin mutation and mycobacterial infection is similar in zebrafish and mice

We analyzed whether leptin mutation and mycobacterial infection caused similar metabolic effects in zebrafish and mice (**Supplementary Table S1**). By applying either a *p* value or a FC filter, 9 metabolites were changed in the same pattern in zebrafish larvae and mice in response to infection in the leptin mutant and wild type (**Table 1**). There were 4 metabolites of which the level was no longer significantly changed in the leptin mutant after infection in both zebrafish larvae and mice (**Table 1**). The 4 metabolites were methionine, asparagine, isoleucine and tryptophan. In conclusion, the metabolic effects caused by leptin mutation and mycobacterial infection are highly conserved in zebrafish larvae and mice.

Metabolite	Infected *vs* control			
	Zebrafish		Mice	
	lepb $^{+/+}$	*lepb* $^{-/-}$	WT	*ob/ob*
Glycine	↓	↓	↓	✕
Histidine	↓	↓	↓	✕
Leucine	↓	↓	↓	✕
Threonine	↓	↓	↓	✕
Cysteine	↓	↓	↓	✕
Methionine	↓	✕	↓	✕
Asparagine	↓	✕	↓	✕
Isoleucine	↓	✕	↓	✕
Tryptophan	↓	✕	↓	✕

Table 1. The changes of 9 common metabolites in response to infection between the wild type and leptin mutant in zebrafish larvae and mice. ↑p<0.05, upregulated, FC<1.5; ↓p<0.05, downregulated, |FC|>1.5; ↓p<0.05, downregulated, |FC|<1.5; ✕ nonsignificant.

## Deep sequencing of transcriptome response to infection of *lepb*⁻/⁻ and *lepb*⁺/⁺ zebrafish larvae

We investigated the transcriptomic profiles of *lepb* mutation and wild type siblings in the absence and presence of *M. marinum* infection in zebrafish larvae by using RNAseq (**Figure 7A** and **B**). Using significance cutoffs of *p*<0.05 and 1.5-fold change (FC), the results showed that the mRNA levels of 1009 genes were significantly changed in *lepb*⁺/⁺ infected zebrafish larvae compared to the *lepb*⁺/⁺ uninfected control (**Figure 7C**). Using the same *p* and FC cutoff values, the result showed that the mRNA levels of 1648 genes were significantly changed in *lepb*⁻/⁻ infected zebrafish larvae compared to the *lepb*⁻/⁻ uninfected control (**Figure 7C**). The number of differentially expressed genes (DEGs) in the *lepb*⁻/⁻ larvae in response to infection was therefore higher than in the *lepb*⁺/⁺ larvae (**Figure 7C**). The Venn diagram of Figure 7C showed 151 common genes in the two signature gene sets. Gene ontology (GO) enrichment analysis using DAVID resulted in significantly (*p*<0.05) enriched GO terms for biological process of the three different groups in the Venn diagram of Figure 7C (**Supplementary Figure S3A** and **S3B**). The significantly enriched GO terms of the 151 common genes include "response to bacterium" and "inflammatory response" (**Supplementary Figure S3B**). In Figure 7D, we illustrated the FC and *p* value of the three groups of genes, shown in Figure 3C, belonging to these two GO terms. A few genes, namely *il1b, il12a, cxl34a.4, saa, irg1l, mmp9* and *cebpb*, were significantly upregulated by infection in the common 151 signature set (**Figure 7D**). More genes related to chemokine signaling were significantly changed in *lepb*⁺/⁺ compared to *lepb*⁻/⁻ larvae after infection. However, the number of significantly regulated genes related to cytokine signaling, the complement cascade and matrix remodeling was higher in *lepb*⁻/⁻ than in *lepb*⁺/⁺ larvae after infection (**Figure 7D**).

Figure 7 (following page). Transcriptome signature sets of *lepb*⁻/⁻ and *lepb*⁺/⁺ zebrafish larvae in the absence and presence of *M. marinum* infection. A. A volcano plot of the signature set of *lepb*⁺/⁺ infected larvae compared to the *lepb*⁺/⁺ uninfected control. We used *p*<0.05 and |FC|>1.5 as cutoff values for all the figures. **B.** A volcano plot of the signature set of *lepb*⁻/⁻ infected larvae compared to the *lepb*⁻/⁻ uninfected control. **C.** A Venn diagram shows the number of differentially expressed genes (DEGs) in response to infection in the *lepb*⁺/⁺ and *lepb*⁻/⁻ larvae. **D.** The FC and *p* value of the three groups of genes, shown in Figure 7C, belonging to the two GO terms "response to bacterium" and "inflammatory responses". **E.** A volcano plot of the signature set of *lepb*⁻/⁻ compared to *lepb*⁺/⁺ larvae in the uninfected control situation. **F.** A volcano plot of the signature set of *lepb*⁻/⁻ compared to *lepb*⁺/⁺ larvae in the infected situation. **G.** A Venn diagram shows the number of DEGs between the *lepb*⁻/⁻ and *lepb*⁺/⁺ in the uninfected

control and infected conditions. **H**. The FC and *p* value of the three groups of genes, shown in Figure 7G, belonging to the two GO terms "response to bacterium" and "inflammatory responses".
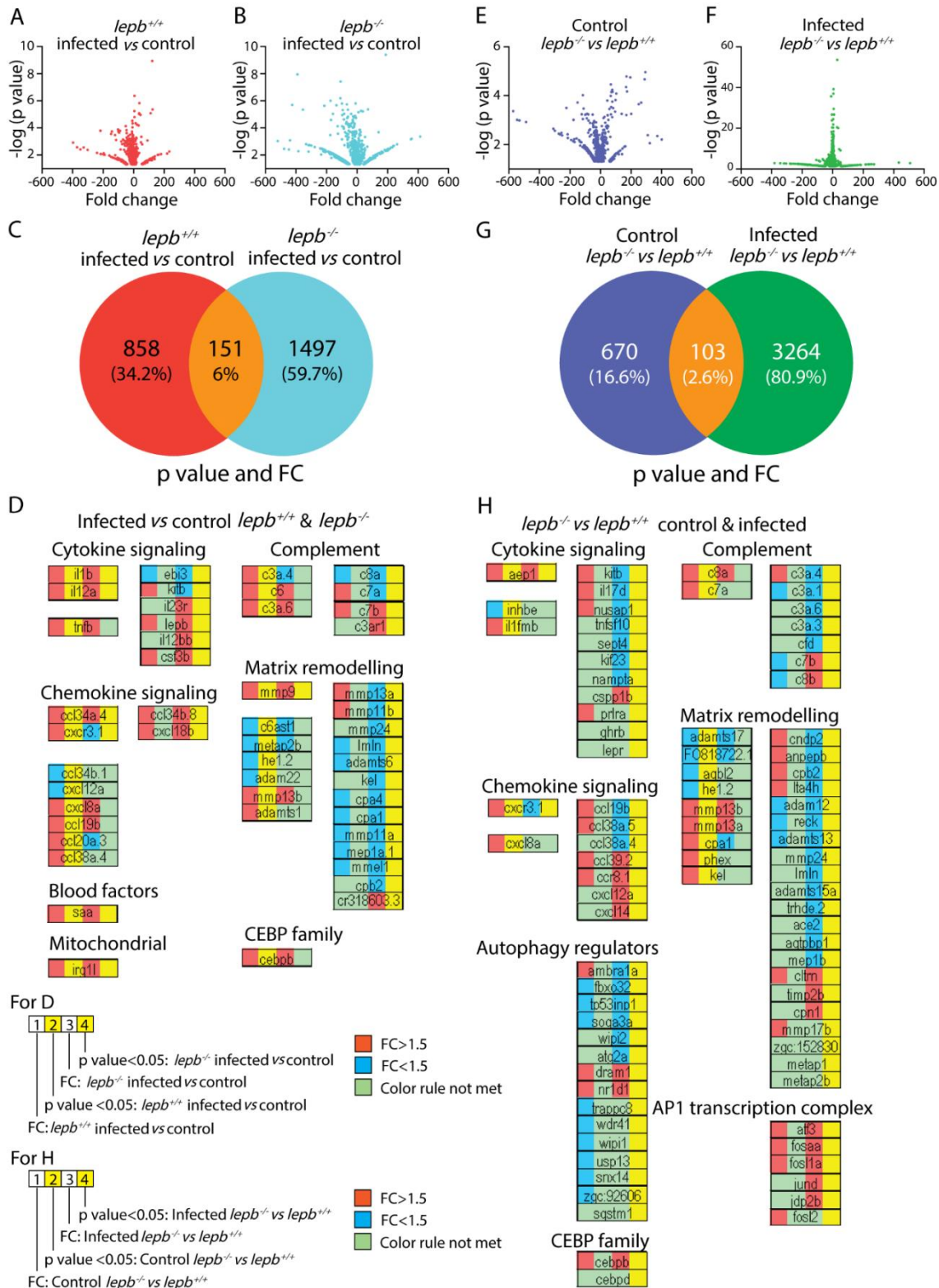
Next, we compared the number of genes that are differentially regulated between the mutant and the wild type in the absence of infection (see volcano plot **Figure 7E**) with the number of differentially regulated genes in the presence of infection (see volcano plot **Figure 7F**). There were 773 genes differentially regulated in the absence of infection at $p<0.05$ and 1.5-FC (**Figure 7G**). However, there were 3367 genes differentially regulated at the same p value and FC cutoff in infected $lepb^{-/-}$ larvae compared to infected $lepb^{+/+}$ siblings (**Figure 7G**). The two signature sets encompassing 773 and 3367 genes showed an overlap of 103 genes (**Figure 7G**). In Figure 7H, we illustrated the FC and p value of the three groups of genes, shown in **Figure 7G**, belonging to the two GO terms "response to bacterium" and "inflammatory response". In the uninfected condition, there were 16 genes differentially regulated between the mutant and the wild type with these GO terms, whereas in the infected condition there were 70 genes (**Figure 7H**). In conclusion, the mutation of the $lepb$ gene and $M.$ $marinum$ infection cause synergistic effects in the transcription of inflammation related genes. We also performed the same comparisons with the genes in glycolysis and gluconeogenesis pathway because of the finding of the metabolomic analysis (**Figure 8**). The result showed that only a few genes were differentially expressed after infection in both the mutant and the wild type (**Figure 8A**). $PCK1$, a key marker for gluconeogenesis, was significantly upregulated in $lepb^{+/+}$ infected group, whereas it was not significantly changed in the $lepb^{-/-}$ infected group (**Figure 8A**). In the uninfected condition, there were no genes differentially regulated between the mutant and the wild type in this pathway, whereas in the infected condition there were 14 genes (**Figure 8B**). In addition, $PCK1$ was significantly lower in the infected $lepb^{-/-}$ larvae compared to infected $lepb^{+/+}$ larvae (**Figure 8B**).

Figure 8 (following page). Genes regulated in glycolysis and gluconeogenesis pathway. A. The differentially expressed genes (DEGs) in response to infection in the $lepb^{+/+}$ and $lepb^{-/-}$ larvae. **B.** The DEGs between the $lepb^{-/-}$ and $lepb^{+/+}$ in the uninfected control and infected conditions.

Leptin mutation and mycobacterial infection leads non-synergistically to a similar metabolic syndrome
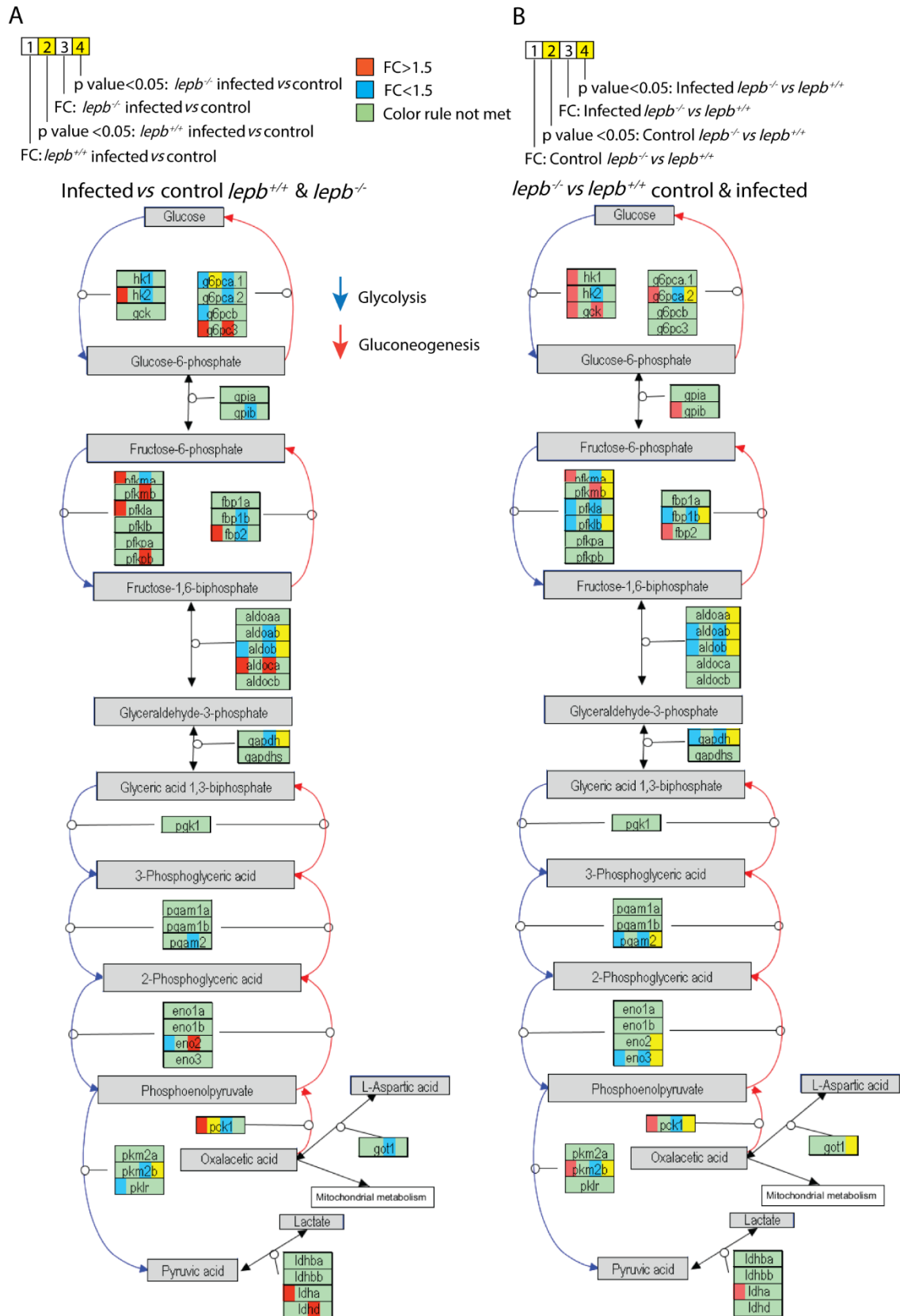
Discussion

In this study, we studied the connections between the role of leptin in TB and T2DM. Therefore, we investigated the effects of mycobacterial infection in leptin deficient *lepb*^{-/-} mutant zebrafish larvae and *ob/ob* mutant mice using metabolomics and transcriptomic techniques. We observed that there were higher bacterial loads in the lungs of *ob/ob* mice infected with *M. tuberculosis* (*Mtb*) bacteria, compared to the wild type infected controls (**Figure 4A**). This observation is consistent with infection studies in *ob/ob* and leptin receptor (*db/db*) mutant mice. Wieland et al. [20] observed a remarkably higher *Mtb* load in the lungs of *ob/ob* mice in comparison with the wild type controls after 5 and 10 weeks of infection. Lemos et al. [26] made the same observation in *db/db* mice infected with *Mtb*. Leptin signaling was also shown to play a key role in macrophage infection by other pathogens such as *Salmonella* Typhimurium [27]. However, since in the study of Fischer et al [27], *lepr* ablation reduced bacterial burden, this indicates that leptin signaling might play a different role in defense towards infections by different species of microbes. For this study, we have used the zebrafish larval model infection system, which has the advantage of a non-feeding system in which the functional adaptive immune system is not yet present and therefore simplifies studies of the innate immune and metabolic responses to infection. Interestingly, we found that there were also higher mycobacterial loads in the *lepb*^{-/-} mutant zebrafish larvae compared to the wild type siblings (**Figure 1B**). This shows that *lepb*^{-/-} mutant zebrafish larvae recapitulate the mice *ob/ob* and *db/db* phenotypes of susceptibility towards mycobacteria infection.

We found that leptin mutation and mycobacterial infection lead to a similar metabolic syndrome in zebrafish larvae as well as in mice (**Table 1**). This similarity could be explained by the occurrence of wasting syndrome in both the leptin mutants and during tuberculosis [5, 19]. In addition to wasting syndrome, *ob/ob* mice exhibit a phenotype of hyperglycemia, similar to human T2DM patients, indicating that leptin plays an important role in regulating glucose metabolism [28]. Plasma leptin level is reduced in conditions of prolonged fasting [29] and leptin has been shown to be a key factor during starvation [18]. In this study, we found that there were significantly higher glucose levels in the *lepb*^{-/-} mutant zebrafish larvae as well as in the condition of *M. marinum* infection (**Supplementary table S1**). *Pck1*, a marker of gluconeogenesis, was observed to be upregulated after infection in the wild type but not in the *lepb*^{-/-} mutant (**Figure 8A**). Consistently, we found that *pck1* expression was lower in the infected *lepb*^{-/-} mutant compared with the infected *lepb*^{+/+} siblings (**Figure 8B**). The expression levels of several other genes in the infected group associated with the glycolysis pathway (**Figure 8B**) were also found to be lower in the *lepb*^{-/-} mutant than in the wild type. Considering the lack of knowledge on the control of gluconeogenesis by infection and leptin signaling, it is hard to speculate on the relevance of these differences of the transcriptional responses of the *lepb*^{-/-} mutant to infection. In any case, it is possible that the higher bacterial loads in the infected *lepb*^{-/-} group lead to extreme limitations of carbon sources for

gluconeogenesis and thereby might have triggered feed-back mechanisms. In support of this hypothesis, the decrease of the levels of many amino acids in the *lepb$^{-/-}$* mutant zebrafish larvae and *ob/ob* mutant mice indicates that the supply of the glucogenic amino acids in the mutants is limiting.

However, in both species, the decrease in the levels of amino acids is not getting more pronounced when the leptin mutant is infected by mycobacteria. We only see very few metabolites, namely trimethylamine N-oxide (**Figure 2D**), mannose (**Figure 3C**), 3-aminoisobutyric acid (**Figure 5B**) and putrescine (**Figure 6C**) of which the levels are changed more severely in the leptin mutant zebrafish larvae and mice in the presence of infection as compared to the wild type. Therefore, we conclude that leptin and mycobacterial infection are non-synergistically controlling metabolism, but lead to a similar metabolic reprogramming. Nevertheless, it is possible that after infection of the leptin mutants as compared to the wild types, more energy is drained from long term storage supplies or depletion of muscle mass, as observed in severe wasting syndrome. This could explain the difference in responses of the *lepb$^{-/-}$* mutant to infection found at the transcriptome level.

At the transcriptome level in zebrafish larvae, we observed that the number of genes of which the expression was significantly changed following *M. marinum* infection was higher in the *lepb$^{-/-}$* mutant than in the sibling control (**Figure 7A**, **B** and **C**). GO term enrichment analysis shows that in both the *lepb$^{-/-}$* mutant and wild type siblings, inflammatory responses to infection were highly enriched (**Supplementary Figure S3**). However, there was a larger set of genes associated with inflammation responding to infection in the *lepb$^{-/-}$* mutant than in the sibling control (**Figure 7D**). This larger gene signature set includes genes of various cytokines, chemokines and genes involved in matrix remodeling and the complement cascade. When comparing the number of genes that are differentially expressed between the mutant and the wild type in the absence of infection with the number of differentially expressed genes in the presence of infection, we also observe larger differences (**Figure 7E**, **F** and **G**). In the absence of infection, the difference in transcriptional levels of inflammatory genes between the mutant and wild type is very limited (**Figure 7G** and **H**). In contrast, in the presence of infection many inflammatory genes have a much stronger response in the *lepb$^{-/-}$* mutant than in the wild type siblings. In addition to the cytokines, chemokines and genes involved in matrix remodeling and the complement cascade, we now also observe various genes of the AP1 transcription complex and genes involved in autophagy regulation to be stronger responding in the mutant (**Figure 7H**).

These data are in seeming contrast with the observations that leptin functions as a proinflammatory cytokine and plays a key role in immunity and inflammatory response in immune cells [25, 30]. Therefore, it has been used as an explanation why leptin deficiency leads to increased susceptibility of infection and it is a risk factor for many infectious diseases including TB [31]. Our data shows that the function of leptin is very complex in that mutation of the *lepb* gene in an infection model

leads to a very different signature set for inflammatory responses. Although there are common transcriptional responses that are still functional in the mutant, a particular set of response factors are selectively activated or inhibited. This is very different from what we found with the metabolic basic state and responses to infection in the mutant and wild type.

In summary it has been published that leptin deficiency increases susceptibility towards mycobacterial infection, impairs immune functions and dysregulates inflammatory responses [30, 32, 33]. Many publications indicate that these effects of leptin deficiency could be due to a direct role in controlling cellular immunity. Our results confirm that there is a very different response in many inflammatory genes transcripts after infection in a zebrafish leptin mutant. The effect of the leptin mutation on the response to infection is very specific for a particular gene signature set and is not a general effect on all inflammatory genes. However, at the metabolism level, there is a general effect of the mutation on the levels of glucose and the glycolysis pathway and a pronounced function in metabolic reprogramming related to wasting syndrome. This effect of the mutation is highly similar to the effect of mycobacterial infection and is not synergistic. Therefore, we can conclude that the function of leptin in defense against mycobacteria is highly complex and is likely to be based on control of both inflammatory and system metabolism. Our metabolic and transcriptomic response signature sets of infection in the leptin mutant and wild type controls can assist in further studies of the mechanisms underlying the role of leptin in glucose homeostasis, wasting syndrome and defense against infection. It thereby could provide further insights in the mechanisms of the connections between immunity and systems metabolism that are still poorly understood.

Methods

Mice

Male *ob/ob* mice and lean C57BL/6 wild type (WT) mice were obtained from Charles River Laboratories. Eight mice per group were nasally infected with *Mtb* strain H37Rv and another eight mice per group were mock infected at 6-week age. The mice were kept under standard conditions for 8 weeks in the animal facility of the Leiden University Medical Center (LUMC). Male mice were chosen because metabolic variation due to the hormonal cycle is limited. The mice were kept on a standard-chow diet with ad libitum access to food and water. One *ob/ob* mouse and one WT infected mouse had to be sacrificed at an early stage due to malocclusion. The mice were sacrificed at week 14 and blood, lung and spleen were collected. Mouse serum samples were collected from clotted blood tubes and mixed with pre-heated 80% ethanol at a 1:3 ratio (end concentration: 60% ethanol) in polypropylene screwcap tubes. Samples were heated for 10 min at 90°C and subsequently chilled on ice for 10 minutes before centrifugation at 13.000 rpm for 10 minutes at

4°C. Supernatants were harvested and stored at -80°C for LC-MS analysis. Handling of mice was conducted in compliance with European Community Directive 86/609 for the care and use of laboratory animals and in accordance with the regulations set forward by the LUMC animal care committee.

Zebrafish larvae

Zebrafish were handled in compliance with the local animal welfare regulations and maintained according to standard protocols (http://zfin.org). Zebrafish breeding and embryo collection were performed as described previously [34]. Mutant *lepb*$^{-/-}$ and wild type sibling *lepb*$^{+/+}$ zebrafish lines were generated, screened and raised as described previously [14]. A *lepb* mutant with a 7 base pair deletion encompassing TAGAGGG in exon 2 was used in this study. Zebrafish *lepb*$^{+/+}$ and *lepb*$^{-/-}$ embryos were collecting from 6-month-old wild type and *lepb* mutant parents, respectively. The embryos were injected into yolk with *M. marinum* strain M labelled with mWasabi plasmid pTEC15 vector22 or mock injected with 2% polyvinylpyrrolidone 40 (PVP40) at 4 to 6 hour post fertilization (hpf). *M. marinum* preparation and automatic microinjection were followed by the protocol of a previous study [35, 36]. Zebrafish larvae at 5 days post fertilization (dpf) were collected and stored at -80°C until further analysis. For HR-MAS NMR measurement, 3 replicates of 120 pooled larvae were used and each sample was measured three times to avoid technique issues.

LC–MS/MS

Metabolite levels in mice serum were measured in individual replicates using a targeted LC-MS/MS platform as described before [5]. Subject numbers were randomized and run in 5 batches which included a calibration line, QC samples and blanks. QC samples were analyzed every 10 samples. They were used to assess data quality and to correct for instrument responses.

The amine platform covers amino acids and biogenic amines employing an Accq-Tag derivatization strategy adapted from a previously published protocol [37]. Briefly, 5.0 µL of each sample was spiked with an internal standard solution. Then proteins were precipitated by the addition of MeOH. The supernatant was dried in a speedvac. The residue was reconstituted in borate buffer (pH 8.5) with AQC reagent. 1.0 µL of the reaction mixture was injected into the UPLC-MS/MS system. Chromatographic separation was achieved by an Agilent 1,290 Infinity II LC System on an Accq-Tag Ultra column. The UPLC was coupled to electrospray ionization on a triple quadrupole mass spectrometer (AB SCIEX Qtrap 6500). Analytes were detected in the positive ion mode and monitored in Multiple Reaction Monitoring (MRM) using nominal mass resolution. Acquired data were evaluated using MultiQuant Software for Quantitative Analysis (AB SCIEX, Version 3.0.2). The data are expressed as relative response ratios (target area/ISTD area; unit free) using proper internal standards. For analysis of amino acids, their 13C15N-labeled analogs were used. For other metabolites, the closest-eluting internal standard was employed. In-house developed algorithms were applied using the pooled QC samples to compensate for shifts in the sensitivity of the mass spectrometer over the batches. After quality control correction,

metabolite targets complied with the acceptance criteria of RSDqc < 15%. Using this platform, we were able to identify 41 metabolites in blood samples from mice.

MS data analysis

Data was analyzed using the software package MetaboAnalyst 5.0 [38]. MetaboAnalyst offers the possibility to provide automated data reports which we used for archiving data sets. Default settings were used with log transformation and auto scaling of the data for normalization. Naming of the metabolites is based on reference compounds using standard nomenclature of the human metabolome database (https://hmdb.ca/).

^{1}H HR-MAS NMR measurement of intact zebrafish larvae

Metabolic profiling by ^{1}H HR-MAS NMR spectroscopy was performed as described in a previous study [19]. Zebrafish larvae were carefully transferred to a 4-mm zirconium oxide MAS NMR rotor (Bruker BioSpin GmbH, Germany). As a reference (^{1}H chemical shift at 0 ppm), 10µl of 100mM deuterated phosphate buffer (KD_2PO4, PH=7.0) containing 0.1% (w/v) trimethyl-silylpropanoic acid (TSP) was added to each sample. The rotor was then placed immediately inside the NMR spectrometer.

All HR-MAS NMR experiments were performed on a Bruker DMX 600-MHz NMR spectrometer, which was equipped with a 4-mm HR-MAS dual inverse ^{1}H/^{13}C probe with a magic angle gradient and spinning rate of 6 kHz with a proton resonance frequency of 600MHz. Measurements were carried out at a temperature of 277 K using a Bruker BVT3000 control unit. Acquisition and processing of data were done with Bruker TOPSPIN software 2.1 (Bruker BioSpin GmbH, Germany).

A standard pulse sequence "ZGPR" (from Bruker's pulse program library) with water pre-saturation was used for measuring one-dimensional ^{1}H HR-MAS NMR spectra. Each one-dimensional spectrum was acquired applying a spectral width of 12 kHz, time domain data points of 8k, number of averages of 128, an acquisition time of 170 msec and a relaxation delay of 2 s. All spectra were processed by an exponential window function corresponding to a line broadening of 1 Hz and zero-filled before Fourier transformation. NMR spectra were phased manually and automatically baseline corrected using TOPSPIN 2.1 (Bruker BioSpin GmbH, Germany). The total analysis time (including sample preparation, optimization of NMR parameters, and data acquisition) of ^{1}H HR-MAS NMR spectroscopy for each sample was approximately 20 min.

NMR analysis

The one-dimensional ^{1}HR-MAS NMR spectra were corrected for baseline, phase shifts and reference using TOPSPIN 2.1 (Bruker BioSpin GmbH, Germany). Subsequently, the spectra were subdivided in the range between 0 and 10 ppm into buckets of 0.04 ppm using MestReNova software version 11.0 (Mestrelab Research S.L., Santiago de Compostela, Spain). The resulting data matrix was saved as the format of script: NMR CSV matrix (transposed) (*.CSV, *.txt). This was

then imported into MetaboAnalyst 5.0 for multivariate analysis using Partial Least Squares Discriminant Analysis (PLS-DA). Correlation coefficients with $p<0.05$ were considered statistically significant. Quantification of metabolites was performed using Chenomx NMR Suite 8.6 (Edmonton, Alberta, Canada), which allowed for qualitative and quantitative analysis of an NMR spectrum by fitting spectral signatures from HMDB database to the respective spectrum. Assignment of peaks was based on the chemical shifts of compounds of interest in Chenomx software. Statistical analysis (t-tests) of the NMR quantification results was performed with GraphPad Prism 8.0.1 (San Diego, CA, USA) and $p<0.05$ were considered significant.

RNA isolation

Zebrafish larvae from $lepb^{+/+}$ and $lepb^{-/-}$ infected and control groups (n=3) were resuspended and crushed in 0.5 ml of TRIzol Reagent. Subsequently, total RNA was extracted in accordance with the manufacturer's instructions. Contaminating genomic DNA was removed using DNase I digestion for 15min at 37°C. RNA concentration was determined by NanoDrop 2000 (Thermo Scientific, the Netherlands). RNA integrity (RIN) was assessed by bioanalyzer (Agilent) and samples with RIN values>6 were used for further library construction and sequencing.

Deep sequencing of zebrafish larvae

Deep sequencing of the zebrafish larvae was performed by GenomeScan B.V. (Leiden, the Netherlands). The NEBNext Ultra II Directional RNA Library Prep Kit for Illumina (NEB #E7760S/L) was used to process the samples. Briefly, mRNA was isolated from total RNA using oligo-dT magnetic beads. After fragmentation of the mRNA, a cDNA synthesis was performed. This was used for ligation of the sequencing adapters and PCR amplification of the resulting product. The quality and yield after sample preparation was measured with Fragment Analyzer. The size of the resulting products was consistent with the expected size distribution (a broad peak between 300-500 bp). Clustering and DNA sequencing using the NovaSeq6000 was performed according to manufacturer's protocols. A concentration of 1.1 nM of DNA was used. For the zebrafish larval samples, data sets of paired end reads of 150 nucleotides were obtained with at least 20 million reads of reads that could be mapped to the zebrafish genome version GRCz11.

Deep sequencing data mapping and analysis

Sequencing data of zebrafish larvae were aligned and mapped to the zebrafish genome GRCz11 using CLC Genomics, and differential gene expression was analyzed using DESeq2 v1.21.1. Gene Ontology (GO) term enrichment and KEGG pathway analysis were performed in DAVID Bioinformatics Resources 6.8 (https://david.ncifcrf.gov/).

Ethical licenses

Experiments in mice were performed under ethical license number DEC 14080 (10-07-2014) of Leiden University. Zebrafish lines were handled in accordance with the local animal welfare regulations and maintained according to standard protocols (https://zfin.org). This local regulation

serves as the implementation of Guidelines on the protection of experimental animals by the Council of Europe, Directive 86/609/EEC, which allows zebrafish embryos to be used up to the moment of free-living (5 days after fertilization). Since embryos used in this study were no more than 5 days old, no license is required by the Council of Europe (1986), Directive 86/609/EEC or the Leiden University ethics committee.

References

[1]   World Health Organization. Global Tuberculosis Report. 2020.

[2]   Kiazyk S, Ball TB. Latent tuberculosis infection: An overview. Can Commun Dis Rep 2017;43(3-4):62-6.

[3]   Paton NI, Ng YM. Body composition studies in patients with wasting associated with tuberculosis. Nutrition (Burbank, Los Angeles County, Calif) 2006;22(3):245-51.

[4]   Weiner J, Maertzdorf J, Sutherland JS, Duffy FJ, Thompson E, Suliman S, et al. Metabolite changes in blood predict the onset of tuberculosis. Nature Communications 2018;9(1):5208.

[5]   Ding Y, Raterink R-J, Marín-Juez R, Veneman WJ, Egbers K, van den Eeden S, et al. Tuberculosis causes highly conserved metabolic changes in human patients, mycobacteria-infected mice and zebrafish larvae. Scientific Reports 2020;10(1):11635.

[6]   Deng J, Liu L, Yang Q, Wei C, Zhang H, Xin H, et al. Urinary metabolomic analysis to identify potential markers for the diagnosis of tuberculosis and latent tuberculosis. Archives of Biochemistry and Biophysics 2021;704:108876.

[7]   Vrieling F, Alisjahbana B, Sahiratmadja E, van Crevel R, Harms AC, Hankemeier T, et al. Plasma metabolomics in tuberculosis patients with and without concurrent type 2 diabetes at diagnosis and during antibiotic treatment. Scientific Reports 2019;9(1):18669.

[8]   Dooley KE, Chaisson RE. Tuberculosis and diabetes mellitus: convergence of two epidemics. Lancet Infect Dis 2009;9(12):737-46.

[9]   Restrepo Blanca I, Schlossberg D. Diabetes and Tuberculosis. Microbiol Spectr 2016;4(6):4.6.48.

[10]   Andrade BB, Kumar NP, Sridhar R, Banurekha VV, Jawahar MS, Nutman TB, et al. Heightened Plasma Levels of Heme Oxygenase-1 and Tissue Inhibitor of Metalloproteinase-4 as Well as Elevated Peripheral Neutrophil Counts Are Associated With TB-Diabetes Comorbidity. Chest 2014;145(6):1244-54.

[11]   Ronacher K, Joosten SA, van Crevel R, Dockrell HM, Walzl G, Ottenhoff THM. Acquired immunodeficiencies and tuberculosis: focus on HIV/AIDS and diabetes mellitus. Immunological Reviews 2015;264(1):121-37.

[12]   Salgado-Bustamante M, Rocha-Viggiano AK, Rivas-Santiago C, Magaña-Aquino M, López JA, López-Hernández Y. Metabolomics applied to the discovery of tuberculosis and diabetes mellitus biomarkers. Biomarkers in Medicine 2018;12(9):1001-13.

[13]   Vrieling F, Ronacher K, Kleynhans L, van den Akker E, Walzl G, Ottenhoff THM, et al. Patients with Concurrent Tuberculosis and Diabetes Have a Pro-Atherogenic Plasma Lipid Profile. EBioMedicine 2018;32:192-200.

[14]   He J, Ding Y, Nowik N, Jager C, Eeza MNH, Alia A, et al. Leptin deficiency affects glucose homeostasis and results in adiposity in zebrafish. Journal of Endocrinology 2021;249(2):125-34.

[15]   Giesbertz P, Padberg I, Rein D, Ecker J, Höfle AS, Spanier B, et al. Metabolite profiling in plasma and tissues of ob/ob and db/db mice identifies novel markers of obesity and type 2 diabetes. Diabetologia 2015;58(9):2133-43.

[16]   Tups A, Benzler J, Sergi D, Ladyman SR, Williams LM. Central Regulation of Glucose Homeostasis. Comprehensive Physiology 2017:741-64.

[17]   Michel M, Page-McCaw PS, Chen W, Cone RD. Leptin signaling regulates glucose homeostasis, but not adipostasis, in the zebrafish. Proceedings of the National Academy of Sciences 2016;113(11):3084-9.

[18]   Perry RJ, Wang Y, Cline GW, Rabin-Court A, Song JD, Dufour S, et al. Leptin Mediates a Glucose-Fatty Acid Cycle to Maintain Glucose Homeostasis in Starvation. Cell 2018;172(1):234-48.e17.

[19]   Alia; Herman P. Spaink YDMCHGF-CJHNNACHTHMNHEJMA. Metabolomic and transcriptomic profiling of adult mice and larval zebrafish leptin mutants reveal a common pattern of changes in metabolites and signaling pathways. Cell & Bioscience 2021.

[20]   Wieland CW, Florquin S, Chan ED, Leemans JC, Weijer S, Verbon A, et al. Pulmonary Mycobacterium tuberculosis infection in leptin-deficient ob/ob mice. International Immunology 2005;17(11):1399-408.

[21]   Soh AZ, Tan CTY, Mok E, Chee CBE, Yuan JM, Larbi A, et al. Adipokines and the risk of active TB: a nested case-control study. The international journal of tuberculosis and lung disease : the official journal of the International Union against Tuberculosis and Lung Disease 2021;25(1):31-5.

[22]   Ye M, Bian L-F. Association of serum leptin levels and pulmonary tuberculosis: a meta-analysis. J Thorac Dis 2018;10(2):1027-36.

[23]   van Crevel R, Karyadi E, Netea MG, Verhoef H, Nelwan RHH, West CE, et al. Decreased Plasma Leptin Concentrations in Tuberculosis Patients Are Associated with Wasting and Inflammation. The Journal of Clinical Endocrinology & Metabolism 2002;87(2):758-63.

[24]   Mansour O, Khames A, I. Radwan E, Yousif M, Elkhatib M. Study of serum leptin in patients with active pulmonary tuberculosis. Menoufia Medical Journal 2019;32(1):217-20.

[25]   Pérez-Pérez A, Sánchez-Jiménez F, Vilariño-García T, Sánchez-Margalet V. Role of Leptin in Inflammation and Vice Versa. International Journal of Molecular Sciences 2020;21(16).

[26]   Lemos MP, Rhee KY, McKinney JD. Expression of the Leptin Receptor outside of Bone Marrow-Derived Cells Regulates Tuberculosis Control and Lung Macrophage MHC Expression. The Journal of Immunology 2011;187(7):3776.

[27]   Fischer J, Gutièrrez S, Ganesan R, Calabrese C, Ranjan R, Cildir G, et al. Leptin signaling impairs macrophage defenses against Salmonella Typhimurium. Proc Natl Acad Sci U S A 2019;116(33):16551-60.

[28]   Wang B, Chandrasekera PC, Pippin JJ. Leptin- and leptin receptor-deficient rodent models: relevance for human type 2 diabetes. Curr Diabetes Rev 2014;10(2):131-45.

[29]   Sonnenberg GE, Krakower GR, Hoffmann RG, Maas DL, Hennes MMI, Kissebah AH. Plasma Leptin Concentrations during Extended Fasting and Graded Glucose Infusions: Relationships with Changes in Glucose, Insulin, and FFA. The Journal of Clinical Endocrinology & Metabolism 2001;86(10):4895-900.

[30]   Maurya R, Bhattacharya P, Dey R, Nakhasi HL. Leptin Functions in Infectious Diseases. Frontiers in Immunology 2018;9:2741.

[31]   Maurya R, Bhattacharya P, Dey R, Nakhasi HL. Leptin Functions in Infectious Diseases. Frontiers in immunology 2018;9:2741-.

[32]   Iikuni N, Lam QLK, Lu L, Matarese G, La Cava A. Leptin and Inflammation. Curr Immunol Rev 2008;4(2):70-9.

[33]   Lord GM, Matarese G, Howard JK, Baker RJ, Bloom SR, Lechler RI. Leptin modulates the T-cell immune response and reverses starvation-induced immunosuppression. Nature 1998;394(6696):897-901.

[34]   Avdesh A, Chen M, Martin-Iverson MT, Mondal A, Ong D, Rainey-Smith S, et al. Regular care and maintenance of a zebrafish (Danio rerio) laboratory: an introduction. J Vis Exp 2012(69):e4196-e.

[35]   Au - Benard EL, Au - van der Sar AM, Au - Ellett F, Au - Lieschke GJ, Au - Spaink HP, Au - Meijer AH. Infection of Zebrafish Embryos with Intracellular Bacterial Pathogens. JoVE 2012(61):e3781.

[36]   Spaink HP, Cui C, Wiweger MI, Jansen HJ, Veneman WJ, Marín-Juez R, et al. Robotic injection of zebrafish embryos for high-throughput screening in disease models. Methods 2013;62(3):246-54.

[37]   Noga MJ, Dane A, Shi S, Attali A, van Aken H, Suidgeest E, et al. Metabolomics of cerebrospinal fluid reveals changes in the central nervous system metabolism in a rat model of multiple sclerosis. Metabolomics 2012;8(2):253-63.

[38]   Pang Z, Chong J, Zhou G, de Lima Morais DA, Chang L, Barrette M, et al. MetaboAnalyst 5.0: narrowing the gap between raw spectra and functional insights. Nucleic acids research 2021.

Supplementary materials
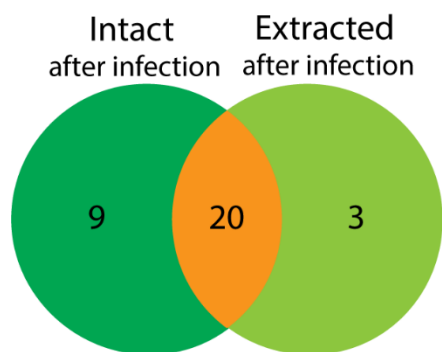
Supplementary Figure 1. Comparison of the number of biomarkers in intact and extracted zebrafish larvae due to *M. marinum* infection. A Venn diagram is shown of the overlap of the 20 metabolites of Intact wild type zebrafish larvae after *M.marinum* infection measured by HR-MAS NMR in this study with the set of infection biomarkers in extracted zebrafish larvae measured by solution NMR published by Ding et al, 2020.
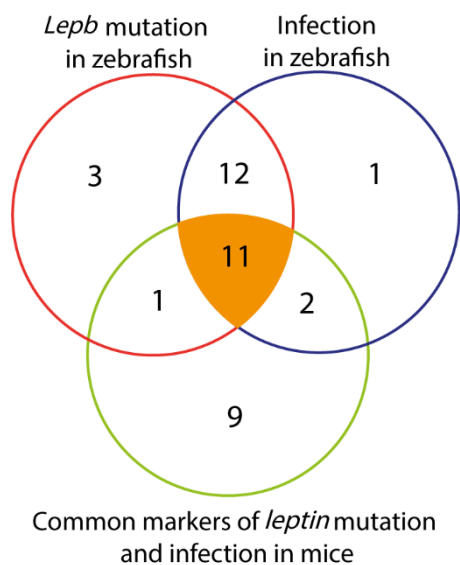
Supplementary Figure 2. Common biomarkers for leptin mutation and mycobacteria infection in zebrafish larvae and mice. A Venn diagram shows that 11 common metabolites are significantly changed in both leptin mutation and mycobacteria infection in zebrafish larvae and mice. Common biomarkers of leptin mutation and infection in mice are from Ding et al, 2021. The 11 common metabolites are alanine, citrulline, ethanolamine, glycine, histidine, isoleucine, leucine, methionine, phenylalanine, serine and threonine. Three anti-correlated metabolites namely ATP, tyrosine and tryptophan are excluded.

A

lepb$^{+/+}$ infected *vs* control   *lepb$^{-/-}$* infected *vs* control

858 (34.2%)   151 6%   1497 (59.7%)

p value and FC
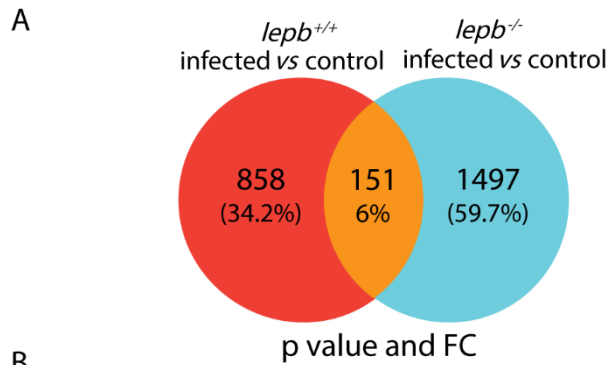
B

Infection signature *lepb +/+* specific	Common genes	Infection signature *lepb -/-* specific
Axon development	Response to bacterium	Transport
Chemokine-mediated signaling pathway	Proteolysis	Proteolysis
Muscle contraction	Glycine biosynthetic process, by transamination of glyoxylate	Thrombin receptor singaling pathway
Neutrophil chemotaxis	Negative regulation of apoptotic process	Axon extension involved in axon guidance
Monocyte chemotaxis	Regulation of mitotic cell cycle	Cellular response to peptide hormone stimulus
Lymphocyte chemotaxis	Protein autophosphorylation	Glucocorticoid biosynthetic process
Cellular response to interferon-gamma	Inflammatory response	Collagen fibril organization
JAK-STAT cascade	Leukocyte migration	Cortisol metabolic process
Cellular response to interleukin-1	Inflammatory response to wounding	Ion transport
lar response to tumor necrosis	Fin regeneration	Potassium ion import
Base-excision repair	Response to molecule of bacterial origin	Roundabout signaling pathway
Cilium organization	Defense response to bacterium	Secondary metabolite biosynthetic process
Bone mineralization	Response to exgenous dsRNA	Response to steroid hormone
Inflammatory response		Cell recognition
Positive regulation of ERK1 and ERK2 cascade		Cholesterol metabolic process
Homophilic cell adhesion via plasma membrane adhesion molecules		Potassium ion transport
		Regulation of axonogenesis
		Cell development
		SMAD protein signal transduction
		Blood coagulation
		Negative regulation of axon extension involved in axon guidance

Supplementary Figure S3. A Venn diagram and GO terms. **A**. A Venn diagram shows the number of differentially expressed genes (DEGs) in response to infection in the *lepb$^{+/+}$* and *lepb$^{-/-}$* larvae with $p<0.05$ and 1.5-FC. **B**. Gene ontology (GO) enrichment analysis using DAVID resulted in significantly ($p<0.05$) enriched GO terms for biological process of the three different groups in the Venn diagram of Supplementary Figure S3A.

Supplementary table S1

Metabolite	$Lepb^{+/+}$_infected vs control		$Lepb^{-/-}$_infected vs control		Control_$lepb^{-/-}$ vs $lepb^{+/+}$		Infected_$lepb^{-/-}$ vs $lepb^{+/+}$	
	FC	p value	FC	p value	FC	p value	FC	p value
2-Aminobutyrate	-1.25	*	-1.12	ns	-1.13	ns	-1.01	ns
Acetate	-2.08	**	-1.04	ns	-2.02	**	-1.01	ns
Alanine	-2.16	***	-1.54	**	-1.39	*	1.01	ns
Arginine	-1.22	*	-1.47	*	1.29	ns	1.07	ns
Asparagine	-1.40	**	1.04	ns	-1.22	*	1.20	ns
Aspartate	-1.77	****	-1.66	****	-1.33	**	-1.25	*
ATP	-1.13	ns	-1.21	ns	1.38	*	1.29	ns
Choline	-1.74	***	-1.38	*	-1.45	**	-1.15	ns
Citrulline	-1.68	****	-1.60	***	-1.67	****	-1.59	***
Creatine	-1.18	ns	1.01	ns	-1.21	*	-1.02	ns
Cysteine	-1.79	****	-1.27	*	-1.24	*	1.13	ns
Ethanolamine	-1.26	*	-1.35	**	-1.33	*	-1.42	**
Glucose	1.29	*	1.22	**	1.25	*	1.18	*
Glutamate	-1.53	**	-1.24	*	-1.53	**	-1.24	**
Glutamine	-1.75	**	-1.26	**	-1.58	*	-1.14	*
Glycine	-1.60	****	-1.25	*	-1.88	****	-1.47	***
Histidine	-1.89	**	-1.42	****	-1.46	*	-1.10	ns
Isoleucine	-1.42	**	-1.03	ns	-1.26	*	1.10	ns
Kynurenine	-1.06	ns	-1.27	ns	1.81	*	1.50	ns
Lactate	-1.16	ns	1.26	*	-1.41	**	1.03	ns
Leucine	-1.59	**	-1.33	*	-1.38	*	-1.15	*
Lysine	-1.90	*	-1.69	***	-1.14	ns	-1.01	ns
Mannose	-1.32	*	1.00	ns	1.21	*	1.60	***
Methionine	-1.64	**	1.06	ns	-1.39	*	1.25	*
myo-Inositol	-1.92	**	-1.28	*	-1.39	*	1.08	ns
NADH	-1.39	ns	-1.16	ns	1.01	ns	1.21	ns
Phenylalanine	-1.77	**	-1.51	****	-1.47	*	-1.25	*
Putrescine	-1.73	**	-1.31	**	-1.57	**	-1.19	ns
Sarcosine	-1.13	ns	-1.04	ns	-1.00	ns	1.07	ns
Serine	-1.42	**	-1.41	***	-1.26	*	-1.26	*
Taurine	-1.47	***	-1.36	**	-1.18	*	-1.10	ns
Threonine	-1.58	**	-1.37	**	-1.34	*	-1.16	*
Trimethylamine N-oxide	1.21	**	1.65	***	-1.21	*	1.14	ns
Tryptophan	-1.38	*	-1.06	ns	1.73	**	2.24	****
Tyrosine	-1.50	*	-2.03	***	1.55	*	1.15	ns

Supplementary table S1. The fold change and p value of all the 35 quantified metabolites in the four different comparisons in zebrafish larvae. ns, not significant. *$p<0.05$, **$p<0.01$, ***$p<0.001$, ****$p<0.0001$.

Supplementary table S2

Metabolite	WT_infected *vs* control		ob/ob _infected *vs* control		Control_*ob/ob* *vs* WT		Infected_*ob/ob* *vs* WT	
	FC	*p* value	FC	*p* value	FC	*p* value	FC	*p* value
2-aminoadipic acid	-2.53	**	-1.68	ns	-3.11	**	-2.07	**
3-aminoisobutyric acid	1.03	ns	1.13	*	-1.06	ns	1.03	ns
4-hydroxy-proline	-1.13	ns	-1.16	ns	-3.51	****	-3.59	****
Alanine	-1.64	**	-1.19	ns	-1.69	**	-1.22	ns
Alpha-aminobutyric acid	-1.53	**	-1.14	ns	-1.75	**	-1.30	**
Arginine	-1.63	**	1.41	*	-4.36	****	-1.90	***
Asparagine	-1.44	*	-1.10	ns	-1.39	ns	-1.06	ns
Aspartic acid	-1.20	ns	-1.27	ns	1.09	ns	1.02	ns
Citrulline	-1.76	**	-1.21	ns	-2.20	***	-1.51	**
Cysteine	-1.04	*	-1.01	ns	1.01	ns	1.04	ns
Ethanolamine	-1.48	**	-1.21	ns	-1.51	ns	-1.23	ns
Gamma-aminobutyric acid	-1.76	**	-1.34	ns	1.19	ns	1.57	ns
gamma-glutamyl-alanine	-2.13	**	-1.22	ns	-3.38	***	-1.93	**
Glutamic acid	-1.56	*	-1.52	ns	1.01	ns	1.04	ns
Glutamine	-1.20	ns	1.06	ns	-2.43	****	-1.90	***
Glutathione	1.05	ns	1.06	ns	-1.04	ns	-1.04	ns
Glycine	-1.59	**	-1.19	ns	-2.41	****	-1.79	****
Histidine	-1.52	***	-1.06	ns	-2.21	****	-1.55	**
Homoserine	-1.70	**	-1.20	ns	-2.02	***	-1.43	*
Hydroxylysine	-1.34	ns	-1.18	ns	-2.17	***	-1.91	**
Isoleucine	-1.75	**	-1.15	ns	-1.87	**	-1.22	ns
Kynurenine	-1.83	**	-1.15	ns	-2.78	***	-1.74	***
Leucine	-1.82	**	-1.14	ns	-2.07	***	-1.30	ns
Lysine	-1.68	**	-1.28	ns	-2.30	***	-1.75	**
Methionine	-1.58	*	-1.20	ns	-2.38	**	-1.81	***
Methionine sulfoxide	-1.95	**	-1.26	ns	-2.81	***	-1.82	****
Methyldopa	-1.92	**	1.01	ns	-1.99	**	-1.03	ns
O-Phosphoethanolamine	-1.28	ns	-1.54	ns	-1.19	ns	-1.43	ns
Ornithine	-1.94	***	-1.59	*	-1.04	ns	1.18	ns
Phenylalanine	-1.78	**	-1.07	ns	-2.05	**	-1.23	ns
Proline	-1.89	***	-1.05	ns	-2.26	***	-1.26	ns
Putrescine	-1.23	ns	-2.19	ns	-1.69	ns	-3.01	****
Sarcosine	-2.82	***	-1.67	ns	-3.06	***	-1.82	**
Serine	-1.58	***	-1.13	ns	-1.38	ns	1.01	ns
Serotonine	-3.25	ns	-1.17	ns	-4.56	*	-1.64	ns
Spermidine	-2.03	*	-1.80	ns	-2.38	*	-2.11	ns
Taurine	-1.23	ns	-1.26	ns	-1.28	ns	-1.31	ns
Threonine	-1.85	**	-1.29	ns	-2.20	**	-1.54	**
Tryptophan	-2.10	**	-1.05	ns	-2.38	**	-1.19	ns
Tyrosine	-1.94	**	1.44	ns	-2.22	**	1.26	ns
Valine	-1.85	**	-1.21	ns	-2.01	**	-1.31	ns

Supplementary table S2. The fold change and *p* value of all the 41 detectable metabolites in the four different comparisons in mice. ns, not significant. *p<0.05, **p<0.01, ***p<0.001, ****p<0.0001.

Supplementary table S3

Category	Metabolite	Infected *vs* control			
		Zebrafish		Mice	
		lepb ^+/+	*lepb* ^-/-	WT	*ob/ob*
Cat.1	Glycine	↓	↓	↓	✕
	Histidine	↓	↓	↓	✕
	Leucine	↓	↓	↓	✕
	Threonine	↓	↓	↓	✕
	Cysteine	↓	↓	↓	✕
	Methionine	↓	✕	↓	✕
	Asparagine	↓	✕	↓	✕
	Isoleucine	↓	✕	↓	✕
	Tryptophan	↓	✕	↓	✕
Cat.2	Alanine	↓	↓	↓	↓
	Citrulline	↓	↓	↓	✕
	Lysine	↓	↓	↓	✕
	Phenylalanine	↓	↓	↓	✕
	Tyrosine	↓	↓	↓	✕
	Ethanolamine	↓	↓	↓	✕
	Serine	↓	↓	↓	✕
	Arginine	↓	↓	↓	↑
	Sarcosine	✕	✕	↓	✕
	Kynurenine	✕	✕	↓	✕
Cat.3	Putrescine	↓	↓	✕	✕
	Taurine	↓	↓	✕	✕
	Glutamine	↓	↓	✕	✕

Supplementary table S3. The changes of 22 common metabolites in zebrafish and mice in response to infection between the wild type and leptin mutants. ↑ *p<0.05, upregulated, FC<1.5; ↓ *p<0.05, downregulated, |FC|>1.5; ↓ *p<0.05, downregulated, |FC|<1.5; ✕ nonsignificant.